Quantitative CT Attenuation Cut-off Values for Lesion Characterization: Enostoses in Patients Without Malignancy Versus Osteoblastic Metastases in Breast Cancer

Novita Pitri[1], Mathelda Diah Wulandari[1], Dario Agustino Nelwan[2], Patricia Jorisal[1], Ivana Dewi Mulyanto[3], Ratna Sari Wijaya[4]
[1]Department of Radiology, Faculty of Medicine, Universitas Pelita Harapan, Jakarta, Indonesia
[2]Department of Radiology, Faculty of Medicine, Universitas Hasanuddin, Makassar, Indonesia
[3]Department of Nuclear Medicine, Faculty of Medicine, Universitas Pelita Harapan, Jakarta, Indonesia
[4]Faculty of Medicine, Universitas Pelita Harapan, Jakarta, Indonesia

Citation : Pitri, N., Wulandari, M. D., Nelwan, D. A., Jorisal, P., Mulyanto, I. D., & Wijaya, R. S. (2026). Quantitative CT Attenuation Cut-off Values for Lesion Characterization: Enostoses in Patients Without Malignancy Versus Osteoblastic Metastases in Breast Cancer. Medicinus, 15(2), 24–32. https://doi.org/10.19166/med.v15i2.10792
Keywords: enostoses, osteoblastic metastases, breast cancer, hounsfield unit, CT attenuation
Correspondance : Novita Pitri
E-mail : novitapitri1234@gmail.com
Online First : 10 March 2026

Abstract

Background:
Incidental osteoblastic bone lesions detected on CT scans, such as enostoses and osteoblastic metastases, often pose diagnostic challenges, especially in patients with or without a history of breast cancer. Hounsfield unit (HU) attenuation values have been proposed to differentiate these lesions non-invasively, however, variability in cut-off values exists in prior studies.

Methods:
This observational analytic case-control study included adult patients who underwent CT and FDG PET-CT at MRCCC Siloam Semanggi Hospital, Jakarta from 2020 to 2025. Controls were patients with enostoses and no history of malignancy, while cases were breast cancer patients with PET/CT-confirmed osteoblastic metastases. Mean and maximum HU values were measured and analyzed to determine optimal cut-offs.

Result:
Mean and maximum HU values were significantly higher in enostoses than in osteoblastic metastases (mean: 1025 ± 123.66 vs. 449.65 ± 106.93; maximum: 1167.77 ± 106.20 vs. 599.34 ± 134.78; $p < 0.001$). A mean HU cut-off of 692 achieved 100% sensitivity, 98.36% specificity, and an AUC of 0.992. A maximum HU cut-off of 860 showed 79.61% sensitivity, 100% specificity, and an AUC of 0.898.

Conclusions:
Mean and maximum HU values on CT are highly effective for differentiating enostoses from osteoblastic metastases in breast cancer patients.

Introduction

The increased use of computed tomography (CT) has led to the incidental detection of bone lesions, highlighting the need to differentiate between enostoses and osteoblastic bone metastases in newly identified sclerotic lesions, especially in cancer patients. Diagnostic challenges arise when these lesions lack the typical characteristics of benign entities like enostoses or indeterminate lesions. This emphasizes the need for accurate lesion characterization to inform staging, prognosis, and treatment decisions. Indeterminate sclerotic lesions should be further evaluated using 18F-FDG PET/CT

and bone scintigraphy.[1,2] Bone metastases is the most common form of skeletal malignancy, affecting approximately 400,000 individuals annually in the United States.[1]

The most frequent primary tumors leading to bone metastases are lung (44.4%), prostate (19.3%), and breast (12.3%) cancers.[3] In Indonesia, breast cancer ranks as the second most common cancer globally, with 2.3 million new cases reported in 2022.[4] Around 70% of advanced breast cancer patients develop bone metastases, which often result in skeletal-related events (SREs) such as pathological fractures, severe bone pain, bone marrow infiltration, and spinal cord compression.[5] While bone metastases in breast cancer are typically osteolytic, approximately 15-20% present as osteoblastic lesions.[6,7] A study conducted at RSUP Dr. Sardjito (2017–2019) found that 48% of bone metastases from breast cancer were osteolytic, 33% osteoblastic, and 19% mixed.[8]

Enostoses is characterized by a size ranging from 2 mm to 2 cm, a round or elongated shape, homogeneous density, orientation along the long axis of the bone, and radiating spicules with trabeculae forming a brush-like pattern.[9,10] Several studies have shown that CT attenuation values can help distinguish enostoses from osteoblastic metastases. Ulano et al.[1] reported a mean cut-off of 885 HU and a maximum of 1060 HU (AUC 0.976, sensitivity 95%, specificity 96%), while Elangovan et al.[11] reported a mean cut-off of 864 HU and a maximum of 910 HU (sensitivity and specificity 93%). However, attenuation values may vary depending on the type of primary tumor, with prostate cancer lesions potentially exceeding the established cut-off. Focusing on breast cancer patients may yield more clinically relevant and homogeneous cut-off values, given that breast cancer is the most common cause of bone metastases in women.[5]

Although CT is an essential tool for anatomical evaluation, 18F-FDG PET/CT offers functional advantages by detecting bone metastases before anatomical changes become apparent, particularly in breast cancer. Metastatic lesions exhibit increased glucose metabolism, detectable via the standardized uptake value (SUV) on PET/CT. However, limited access and high costs restrict the widespread use of PET/CT. In contrast, CT is more readily available and can serve as a non-invasive alternative for diagnosing bone metastases.[12,13] This study aims to compare CT attenuation values between enostoses and osteoblastic metastases, determine accurate cut-off values, and evaluate the diagnostic performance of CT.

Material And Methods

This is an observational analytical study with a case-control design, aimed at determining the CT attenuation cut-off value (Hounsfield Units) on CT scans and evaluating the diagnostic accuracy for distinguishing enostoses in patients with no cancer history from breast cancer patients with osteoblastic metastases. The study was conducted at the Department of Radiology and Nuclear Medicine at Siloam MRCCC Semanggi, Jakarta, from July to September 2025. Data for this study was collected retrospectively by reviewing radiology and nuclear medicine reports stored in the PACS system and medical records of the patients. The data include patients who have undergone CT or 18F-FDG PET/CT scans and have been diagnosed with either enostoses or osteoblastic metastases, based on the predefined inclusion and exclusion criteria. Patient data will be selected using specific keywords, such as "bone island," "enostoses," "sclerotic focus," "sclerotic lesion," as well as and "osteoblastic metastases,".

Enostoses

The inclusion criteria of the ensotosis group consist of patients aged over 18 years who have sclerotic bone lesions exhibiting typical enostoses morphology. It is characterized by lesions measuring between 2 mm and 2 cm in size, round or elongated in shape, homogeneous in density, oriented along the long axis of the bone, with radiating spicules merging with adjacent trabeculae. The exclusion criteria for this group include patients with a history

of malignancy, sclerotic lesions smaller than 3 mm in diameter, and patients with significant artifacts (beam hardening).

Osteoblastic Metastases

The inclusion criteria of the osteoblastic metastases group include histopathologically confirmed breast cancer patients who present with sclerotic bone lesions on CT scans, which are confirmed by an abnormal avidity increase on 18F-FDG PET/CT. The exclusion criteria for this group are patients who have previously received chemotherapy or radiation therapy, sclerotic lesions smaller than 3 mm in diameter, patients with significant artifacts (beam hardening), and those who did not undergo PET/CT scans using Philips equipment. Osteoblastic metastases lesions will be evaluated using a Philips Gemini TF TOF 16-slice PET/CT scanner with a whole-body protocol, including a slice thickness of 5 mm, tube voltage of 120 kVp, and a table feed of 30 mAs. These lesions will also be reviewed by two radiologists who will provide a consensus interpretation, with final confirmation from a nuclear medicine specialist.

CT Examinations

Enostoses lesions will be assessed using a Philips iBrilliance 256-slice CT scanner, with CT protocols for the thorax, abdomen, and pelvis, employing a slice thickness of 1 mm, tube voltage of 120 kVp, and a table feed of 200 mAs, with a standard body filter for both thorax and pelvis examinations. Similarly, osteoblastic metastases lesions will be evaluated using a Philips Gemini TF TOF 16-slice PET/CT scanner with a whole-body protocol, including a slice thickness of 5 mm, tube voltage of 120 kVp, and a table feed of 30 mAs. Both enostoses and osteoblastic metastases lesions will be reviewed by two radiologists who will provide a consensus interpretation, with final confirmation from a nuclear medicine specialist.

Density measurements for both enostoses and osteoblastic metastases lesions on CT scans will be performed by placing a circle and free-hand region of interest (ROI) on axial slices, ensuring the boundaries of the lesions are not exceeded. Attenuation values will be measured independently by two radiologists using the PACS workstation (Infinite), with bone window settings (window width: 1500 HU; window level: 440 HU). The average and maximum attenuation values for each lesion will be recorded in Hounsfield Units (HU). All measurements will be categorized into two groups based on lesion type: enostoses or osteoblastic metastases.

Statistical Analysis

Data will be systematically recorded on research forms and entered into a database using the Statistical Package for the Social Sciences (SPSS) version 26.0. Univariable analysis will be performed descriptively for both numeric and categorical data. Numeric data, such as age, lesion size, number of lesions, and attenuation values, will first be tested for normality. If the data is normally distributed, an independent t-test will be used to compare groups (enostoses vs osteoblastic metastases). For non-normally distributed data, the Mann-Whitney U test will be applied. A significance level of $p < 0.05$ with a 95% confidence interval will be considered statistically significant.

In order to determine the optimal Housefield Unit (HU) cut-off value for distinguishing between enostoses and osteoblastic metastases, the Youden Index method will be employed based on the Receiver Operating Characteristic (ROC) curve analysis. The area under the curve (AUC) will be calculated, and the sensitivity, specificity, positive predictive value (PPV), and negative predictive value (NPV) will be determined by identifying true positives, true negatives, false positives, and false negatives. All statistical analyses related to these measures will be conducted using MedCalc software.

Result

Subject Charateristics

A total of 56 study subjects were successfully enrolled, consisting of 38 patients with enostoses lesions and 18 patients with metastases lesions. In both groups, a total of 61 enostoses lesions and 103 metastases lesions were identified. The characteristics of the study subjects are presented in Table 1. The distribution of

gender did not differ significantly between the two groups, with a majority of enostoses patients being female (57.9%), while all patients in the metastases group were female (100%). The average age of patients in the enostoses group was 44.7 ± 14.24 years, slightly lower than the metastases group, which had an average age of 53.5 ± 10.9 years, though this difference was not statistically significant (p=0.062). The median number of lesions in the metastases group (4.5; min-max 1–15) was significantly higher compared to the enostoses group (1; min-max 1–5), with a p-value of 0.001, indicating a greater disease burden in the metastases group.

The mean HU value for enostoses lesions was significantly higher, with an average of 984.75 ± 131.29, compared to metastases lesions, which had a mean of 449.37 ± 106.90 (p < 0.001; 95% CI: 490.11–580.63) as seen in Table 2. For the maximum HU value, the enostoses group showed a much higher value of 1149.23 ± 119.89, in contrast to metastases lesions, which had a mean of 599.18 ± 134.83 (p < 0.001; 95% CI: 497.40–602.69). Additionally, the median lesion size in the metastases group (15 mm; min-max 4–72 mm) was significantly larger than in the enostoses group (6 mm; min-max 3–12 mm) with a p-value < 0.001 (95% CI: 3–72). The Mann-Whitney test indicated a significant difference in both lesion density and size between the two groups.

In subgroup analysis for enostoses, the difference in mean HU between males (1009.60 ± 125.82) and females (1035.40 ± 123.19) was not statistically significant (Mann-Whitney p = 0.360), and for maximum HU, the difference between males (1166 ± 93.47) and females (1168.42 ± 114.97) was also not significant (p = 0.626). Statistically, these findings suggest that enostoses density on CT does not differ significantly by gender in this study population, allowing the HU cut-off value to be applied without the need for stratification by sex. Metastases lesions were primarily located in the vertebra (73.8%), pelvis (16.5%), and femur (4.9%), whereas enostoses lesions were more evenly distributed, with the highest prevalence in the pelvis (34.4%) and vertebra (40.6%) as seen in Table 3. Both lesion types were mostly eccentric (metastases: 74.8%, enostoses: 81.3%). Irregular lesion shapes were predominant in metastases (58.3%), while enostoses lesions were all regular.

Radiating spicule margins were more common in enostoses (50%), while metastases lesions had well-defined (48.1%) and ill-defined (58.3%) margins. No periosteal reaction was observed in either group. Regarding lesion density, 93.2% of metastases lesions were heterogeneous, compared to 100% of enostoses lesions being homogeneous. Aggressive features, including periosteal reaction, cortical destruction, soft tissue extension, and pathological fractures, were absent in enostoses. In contrast, osteoblastic metastases exhibited aggressive characteristics: cortical destruction in 68% of cases and pathological fractures in 10.7%, with no periosteal reaction or soft tissue extension observed in this study population. The analysis revealed no significant differences between metastases and non-metastases groups in terms of pathological fractures (p = 0.998), cortical destruction (p = 0.996), lesion density (p = 0.995), lesion shape (regular vs. irregular) (p = 1.000), margin type (radiating vs. well-defined, p = 0.994; ill-defined vs. well-defined, p = 0.993), and transverse location (eccentric vs. central, p = 0.099).

Table 1. Demographic Characteristics of Patients with Enostoses and Metastases Lesions

Variabel	Enostoses (n=38)	Metastases (n=18)	P-value
Sex n (%)*			0.001
Male	16(42.1)	0 (0.0)	-
Female	22 (57.9)	18 (100)	-
Age (mean ± SD) ∞	44.7 ± 14.24	53.5 ± 10.93	<0.001
Number of lesion (median ± min-max)∞	1 ± 1-5	4 ± 1-15	<0.001

SD: Standard Deviation;: T test ; ∞ : Mann-Whitney*

Table 2. Comparison of Mean HU, Maximum HU, and Lesion Size between Enostoses and Metastases and Subgroup Analysis

Variable	Enostoses (n=61)	Metastases (n=103)	P-value
Mean HU (mean ± SD)∞	1025 ± 123.66	449.65± 106.93	<0.001
Maximum HU (mean ± SD)∞	1167.77 ± 106.20	599.34 ± 134.78	<0.001
Size (median ± min-max)∞	7 ± 3-12	19 ± 8-34	<0.001
Enostoses	Male (n =24)	Female (n=37)	P-value
Mean HU (mean ± SD)∞	1009.60 ± 125.82	1035.40 ± 123.19	0.360
Maximum HU (mean ± SD)∞	1166± 93.47	1168.42± 114.97	0.626

∞ : *Mann-Whitney*

Table 3. Radiological Characteristics of Enostoses and Metastases Lesions

Variable	Enostoses (n=32)	Metastases (n=103)
Anatomical Location, n (%)		
Vertebrae	13 (40.6)	76 (73.8)
Pelvis	11 (34.4)	17 (16.5)
Costae	0 (0.0)	1(1.0)
Sternum	0 (0.0)	1(1.0)
Humerus	1 (3.1)	1(1.9)
Femur	6 (18.8)	5 (4.9)
Scapula	1 (3.1)	2 (1.9)
Transverse Location, n (%)		
Centric	6 (18.8)	26 (25.2)
Eccentric	26 (81.3)	77 (74.8)
Shape, n (%)		
Reguler	32 (100)	43(41.7)
Ireguler	0 (0.0)	60 (58.3)
Lesion Margin, n (%)		
Well-defined	16 (50.0)	43(41.7)
Radiating Spicules	16 (50.0)	0 (0.0)
Ill-defined	0 (0.0)	60 (58.3)
Density, n (%)		
Homogenous	32 (100.0)	7 (6.8)
Heterogenous	0 (0.0)	96 (93.2)
Periosteal Reaction, n (%)		
No	32 (100.0)	103 (100.0)
Yes	-	-
Cortex Destruction, n (%)		
No	32 (100.0)	33 (32.0)
Yes	0 (0.0)	70 (68.0)
Soft Tissue Extension, n (%)		
No	32 (100.0)	103 (100.0)
Yes	-	-
Pathological Fracture, n (%)		
No	32 (100.0)	92 (89.3)
Yes	0 (0.0)	11 (10.7)

Diagnostic Accuracy of Mean HU and Maximum HU to Differentiate Enostoses and Metastases Lesions

The cut-off for mean HU ≤ 692 demonstrated 100% sensitivity, 98.36% specificity, 99.03% positive predictive value (PPV), 100% negative predictive value (NPV), and 87.14% accuracy, with an area under the curve (AUC) of 0.992 (95% CI: 0.963–1.000) and a Youden index of 0.9836 (Figure 1 and Table 4). Meanwhile, the cut-off for maximum HU ≤ 860 showed 79.61% sensitivity, 100% specificity, 100% PPV, 97.78% NPV, and 97.96% accuracy, with an AUC of 0.898 (95% CI: 0.841–0.940) and a Youden index of 0.9903. These results highlight the excellent diagnostic performance of HU measurements in differentiating between enostoses and metastases lesions.

Table 4. Cut-off Mean HU Values and Diagnostic Test Results for Differentiating Enostoses and Metastases.

Parameter	Cut-off values	Sensitivity (%)	Spesificity (%)	PPV (%)	NPV (%)	Accuracy (%)	AUC (95%CI)	Youden Index
Mean HU	≤ 692	100.0	98.36	87.14	100	98.25	0.992(0.963–1.000)	0.9836
Max HU	≤ 860	79.61	100	100	97.78	97.96	0.898(0.841–940)	0.9903

HU : Hounsfield unit ; AUC: Area Under The Curve; PPV: Positive Predictive Value; NPV: Negative Predictive Value; CI: Confidence Interval

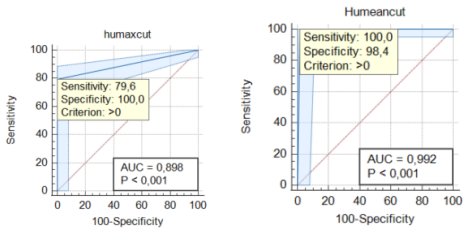

Figure 1. The ROC curve for cut-off mean HU and maximum HU.

Discussion

In this study, the mean HU value for enostotic lesions was significantly higher than that for osteoblastic metastases lesions, with values of 984.75 ± 131.29 versus 449.37 ± 106.90 ($p < 0.001$), indicating a statistically significant difference. This discrepancy suggests that enostotic lesions possess higher bone density, reflecting pathological characteristics of compact, dense, and homogeneous bone composition. In contrast, metastases lesions exhibited lower mean HU values, consistent with their more heterogeneous and invasive nature.[1,2,11] Previous studies by Ulano et al.[1] and Elangovan et al.[11] also reported higher mean HU for enostoses, supporting its use as an effective differentiation parameter. Maximal HU values followed a similar trend, with enostoses showing 1149.23 ± 119.89 HU, significantly higher than metastases (599.18 ± 134.83 HU, $p < 0.001$).

The significant difference in lesion size (median 15 mm for meatstasis vs. 6 mm for enostoses, $p < 0.001$) indicates a heavier disease burden in metastatic patients. This reflects the aggressive nature of the tumor with faster and more invasive growth compared to benign enostoses lesions.[9] Several studies confirm that metastases lesions are typically larger due to active tumor infiltration and proliferation in bone tissue.[1,2,11] These findings align with previous research showing that most enostoses lesions range from 2 mm to 2 cm, although "giant bone islands" greater than 2 cm have also been reported.[10,14]

The study found that most metastases lesions were in the vertebrae, pelvis, followed by femur, while enostoses lesions were more evenly distributed, with the highest prevalence in the pelvis and vertebrae. This supports the idea that metastases occur in highly vascularized areas, while enostoses is more diffusely located.[1,2,11] Transverse location analysis also showed that both metastases and enostoses lesions were predominantly in eccentric areas, which contrasts with previous studies where enostoses was more centrally located. Eccentric lesions in metastases suggest an aggressive growth pattern invading the periosteal and cortical areas, while the centrally located, homogeneous lesions in enostoses indicate a more benign and stable nature.[1,2]

Lesion shapes differed significantly, with metastases showing irregular shapes and ill-defined margins, while enostoses was mostly regular with clear margins and radiating spicules. These radiating spicules that reflects smooth bone trabeculae spread help to differentiate metastases and enostoses.[2,11] Cortical destruction and pathological fractures were found only in metastases, indicating invasion and structural damage typical of malignancy, highlighting CT's role in assessing malignant complications.[15] A study by Slouma et al. showed that osteoblastic metastases, particularly those originating from prostate and breast cancer, exhibit lower metabolic activity, such as reduced cytokine release and related inflammatory processes that stimulate periosteal reactions.[16]

This study found that mean and maximum HU values on CT scans are highly effective diagnostic parameters for distinguishing enostoses from osteoblastic metastases in breast cancer patients. The mean HU cut-off of ≤ 692 showed 100% sensitivity and 96.87% specificity, while the maximum HU cut-off of ≤ 860 showed 99.03% sensitivity and 100% specificity. These findings align with Ulano et al.[1] who showed that both mean and maximum CT attenuation can differentiate enostoses from untreated osteoblastic metastases, with thresholds of 885 HU and 1060 HU, respectively. Sala et al.[2] confirmed that mean HU for enostoses is consistently higher (1007 HU) than for metastases (728 HU), with a cut-off of 881 HU achieving 98% sensitivity and 95% specificity. They also highlighted the importance of considering clinical context and using representative ROI to avoid measurement bias. Our study found lower cut-off values but similarly high accuracy, supporting HU as a valid parameter for breast cancer patients.[2]

These HU cut-off values could reduce the need for biopsies, particularly in cases of sclerotic bone lesions. However, HU interpretation should be considered

alongside clinical and radiological information, as both treatment and imaging techniques can affect HU readings. Differences in HU cut-off values may also be influenced by the type of primary cancer.[17] For example, prostate cancer metastases typically show higher HU due to prostate-specific antigen (PSA) and osteoblastogenesis. In contrast, breast cancer metastases, influenced by parathyroid hormone-related peptide (PTHrP), lead to osteolysis and less dense sclerosis, which is reflected in our lower HU cut-off compared to previous studies. Additionally, treatment effects, such as radiation, can alter HU values and serve as an indicator of treatment response.[18,19]

This study has several limitations. The small sample size and the case-control design may lead to overestimated accuracy. Lesion diagnosis relied on clinical, radiological, and FDG PET/CT criteria rather than histopathology, allowing for potential misclassification. Variations in imaging protocols may also affect HU measurements and lesion morphology. Additionally, the study's focus on breast cancer osteoblastic metastases limits its applicability to other cancers.

Conclusion

The mean and maximum HU values for enostoses were significantly higher than those for metastases ($p < 0.001$), with a mean HU cut-off of ≤ 692 showing 100% sensitivity and 98.36% specificity, and a maximum HU cut-off of ≤ 860 showing 79.61% sensitivity and 100% specificity. These findings suggest that HU values could serve as an effective diagnostic parameter, potentially reducing the need for invasive biopsy and costly additional tests, although further validation in larger, prospective populations with uniform imaging protocols is required.

Acknowledgment

None.

References

1. Ulano A, Bredella MA, Burke P, Chebib I, Simeone FJ, Huang AJ, et al. Distinguishing untreated osteoblastic metastases from enostoses using CT attenuation measurements. Am J Roentgenol. 2016 Aug 1;207(2):362–8.

2. Sala F, Dapoto A, Morzenti C, Firetto MC, Valle C, Tomasoni A, et al. Bone islands incidentally detected on computed tomography: frequency of enostosis and differentiation from untreated osteoblastic metastases based on CT attenuation value. Br J Radiol. 2019;92(1103).

3. Knapp BJ, Cittolin-Santos GF, Flanagan ME, Grandhi N, Gao F, Samson PP, et al. Incidence and risk factors for bone metastases at presentation in solid tumors. Front Oncol. 2024;14.

4. Sung H, Ferlay J, Siegel RL, Laversanne M, Soerjomataram I, Jemal A, et al. Global Cancer Statistics 2020: GLOBOCAN Estimates of Incidence and Mortality Worldwide for 36 Cancers in 185 Countries. CA Cancer J Clin. 2021 May;71(3):209–49.

5. Gong Y, Zhang J, Ji P, Ling H, Hu X, Shao ZM. Incidence proportions and prognosis of breast cancer patients with bone metastases at initial diagnosis. Cancer Med. 2018 Aug 1;7:4156.

6. Kozlow W, Guise TA. Breast cancer metastasis to bone: mechanisms of osteolysis and implications for therapy. J Mammary Gland Biol Neoplasia. 2005 Apr;10(2):169–80.

7. World Cancer Research Fund. Breast cancer statistics [Internet]. World Cancer Research Fund. 2025 [cited 2025 Apr 7]. p. 1–10. Available from: https://www.wcrf.org/preventing-cancer/cancer-statistics/breast-cancer-statistics/

8. Yatulaili F, Poedjomartono B, Dwidanarti SR. Perbedaaan Nilai Densitas Ct Scan Metastasis Tulang Tipe Osteoblastik Pada Pasien Kanker Payudara Dengan Enostosis. Univ Gadjah Mada. 2019;1(1):1–10.

9. Singh Dharmshaktu G, Singh B. Bone island and hand involvement-A short review. Rev Hand Microsurg. 2018;7:93–7.

10. Greenspan A. Bone island (enostosis): current concept--a review. Skeletal Radiol. 1995;24(2):111–5.

11. Elangovan SM, Sebro R. Accuracy of CT Attenuation Measurement for Differentiating Treated Osteoblastic Metastases From Enostoses. AJR Am J Roentgenol. 2018 Mar 1;210(3):615–20.

12. Almuhaideb A, Papathanasiou N, Bomanji J. 18F-FDG PET/CT Imaging In Oncology. Ann Saudi Med. 2011 Jan;31(1):3.

13. Litt HK, Kwon DH, Velazquez AI. FDG PET Scans in Cancer Care. JAMA Oncol. 2023 Sep 1;9(9):1304–1304.

14. Falk GL, Simpson SB. Incidental Benign Skeletal Lesions: Bone Islands. Clin Atlas Bone SPECT/CT. 2023;783–7.

15. Tsurumoto T, Wakebe T, Ogami-Takamura K, Okamoto K, Tashiro K, Saiki K. An Ancient Skeleton with Multiple Osteoblastic Bone Lesions Containing a Scapular Sunburst Appearance from a 5th–6th Century Grave Excavated in Oita, Japan. Biomed Res Int. 2018;2018:1659510.

16. Slouma M, Abbes M, Dhahri R, Gueddiche NE, Msekni I, Gharsallah I, et al. Rectal carcinoma revealed by isolated mixed bone metastases. Clin Case Reports. 2022 Feb;10(2):e05380.

17. Azar A, Garner HW, Rhodes NG, Yarlagadda B, Wessell DE. CT Attenuation Values Do Not Reliably Distinguish Benign Sclerotic Lesions From Osteoblastic Metastases in Patients Undergoing Bone Biopsy. AJR Am J Roentgenol. 2021 Apr 1;216(4):1022–30.

18. Keller ET, Brown J. Prostate cancer bone metastases promote both osteolytic and osteoblastic activity. J Cell Biochem. 2004;91(4):718–29.

19. Logothetis CJ, Lin SH. Osteoblasts in prostate cancer metastasis to bone. Nat Rev Cancer. 2005 Jan;5(1):21–8.

Author's Statement

The authors declared that all the images and figures in this manuscript is/are author's own work and/or has obtained necessary permission to re-use the content from the authors and publisher of respective materials.

(Novita Pitri)